IOPscience iopscience.iop.org

Home Search Collections Journals About Contact us My IOPscience

Thermal decomposition kinetics of amorphous carbon nitride and carbon films

This article has been downloaded from IOPscience. Please scroll down to see the full text article.

2002 J. Phys.: Condens. Matter 14 1697

(http://iopscience.iop.org/0953-8984/14/8/301)

View the table of contents for this issue, or go to the journal homepage for more

Download details:
IP Address: 171.66.16.27
The article was downloaded on 17/05/2010 at 06:11

Please note that terms and conditions apply.

INSTITUTE OF PHYSICS PUBLISHING JOURNAL OF PHYSICS: CONDENSED MATTER
J. Phys.: Condens. Matter **14** (2002) 1697–1708 PII: S0953-8984(02)30258-3

Thermal decomposition kinetics of amorphous carbon nitride and carbon films

Li Hong Zhang[1,2,3], **Hao Gong**[1,4] **and Jian Ping Wang**[2]

[1] Department of Materials Science, National University of Singapore, 119260, Singapore
[2] Data Storage Institute, National University of Singapore, 119260, Singapore

E-mail: masgongh@nus.edu.sg (Hao Gong)

Received 26 October 2001, in final form 29 January 2002
Published 15 February 2002
Online at stacks.iop.org/JPhysCM/14/1697

Abstract
Kinetic thermal degradation of amorphous carbon and carbon nitride films is studied. Significantly improved thermal stability was observed for films intensified with C–N, C=N, and C≡N bonds. When the N_2% (percentage of nitrogen) in Ar/N_2 during film deposition was varied from 0 to 30 at pressures of 3×10^{-3} and 16×10^{-3} Torr, the onset decomposition temperatures increased from 396 to 538 and from 340 to 360 °C, while the apparent activation energy ΔE at 60% residual weight increased from 149 to 158 and from 96 to 120 kJ mol^{-1}, respectively. A change in the thermal stability was observed when the N_2% reached 50. The films of higher bonding ratio and structural integration showed a single-step decomposition mechanism. They had ΔE values decreasing with the decomposition process, following convex-trend isothermal weight-loss curves. Films deposited using low-energy carbon plasma had higher contents of loosely bonded molecules; this resulted in a seemingly two-step decomposition and ΔE increasing with weight loss over a certain range. They followed concave-trend isothermal weight-loss curves. The overall decomposition mechanism could best be expressed in terms of nth-order reactions with the value of n closely related to film structures and reaction temperatures. Lower n-values are related to densely packed structure and higher temperature due to the increased diffusion barrier of the products.

1. Introduction

Amorphous carbon (a-C) and carbon nitride (a-C:N) films are of great interest and importance for a number of tribological and protective applications owing to their properties, such as low friction coefficient, good chemical inertness, high hardness, wide optical band transparency,

[3] Currently at: Seagate Technology International, 01-6 The Fleming, Science Park Drive, Singapore.
[4] Author to whom any correspondence should be addressed.

 © 2002 IOP Publishing Ltd Printed in the UK

and low physical thickness achievable. They are described as a long-range amorphous structures consisting of nanocrystalline graphite crystals dispersed in an amorphous matrix consisting of sp^2- and sp^3-bonded atoms. The properties are more closely related to the degree of short-range order. Nitrogenated amorphous carbon films are synthesized by various methods in order to replace a-C films as the protective coatings of magnetic hard disks. a-C:N films of certain nitrogen content have been reported to show much better wear resistance and long-term wear durability than a-C:H and a-C films. Researchers have performed systematic structure analysis on sputter-coated carbon nitride films and examined their properties on a microstructural basis. To understand the fundamental properties of a-C:N films, some investigations on their electrical, optical, mechanical, and tribological properties have been performed [1–7]. Certain thermal effects on a-C:N films were also identified [2]. However, the reasons for the performance of a-C:N films are still not fully understood. Quantitative thermal information is particularly scarce but is extremely important. It correlates the structural and physicochemical properties with the decomposition mechanisms, kinetics, and stability. The chief value of quantitative thermal information is in helping one to understand the changes in the kinetic parameters with temperature and time, because it is closely related to the fundamental structural composition [1–13].

Thermogravimetry (TG) methods using state-of-art thermal analysers are known to be highly reliable in interpreting the thermal decomposition properties and kinetics of different materials. The dynamic approach studies the weight changes of a material with temperature in various gaseous environments, which reveal the thermal stability of the material and the amounts of foreign materials adsorbed in it. It also tells us the purity of a material if its thermal properties are known [14]. Most TG instruments available record the differential thermogravimetric (DTG) signals, which are the differentials of weight versus temperature curves. DTG plots are useful in differentiating the weight changes when some decomposition steps overlap in a TG curve. Another common approach in TG analysis is the isothermal method, which is useful in interpretation of the complex solid-state decomposition reactions, and gives direct access to the determination of the apparent activation energy on the basis of the Arrhenius equation describing the relationship of the reaction rate and temperature in the chemically controlled reaction region [15]. In an isothermal TG operation, the temperature is quickly raised to the designated temperature ($200\,^{\circ}\mathrm{C\ min^{-1}}$) and the weight changes of a material are recorded over time. From the weight versus time curve, reaction rates can be obtained. A typical thermal decomposition process in an oxidizing atmosphere involves mass transfer, adsorption, desorption, and rearrangement. At low temperatures, the reaction rate is chemically controlled, but it changes to being diffusion controlled at high temperatures, when large amounts of products are decomposed and their diffusion is insufficient [16]. This work studies systematically and quantitatively the thermal kinetics, properties, and stability of a-C:N and a-C films. Their reaction rates, apparent activation energies, and mechanisms, in association with physicochemical structures, are investigated and discussed.

2. Experimental details

Each of the films was deposited on a glass substrate of 0.15 mm thickness using a dc magnetron sputtering system (INNOTEC D28) operating at a dc power of 800 W and a base chamber pressure of 3×10^{-6} Torr, achieved through a cryopump. The glass substrate was ultrasonically cleaned in acetone and methanol and preheated at $400\,^{\circ}\mathrm{C}$ for 1 h before film deposition. Both the high-purity pyrolytic graphite target (99.999%) and the substrate were sputter-cleaned before each deposition. By varying the nitrogen ratio in the sputtering gases (N_2/Ar, both with 99.999% purity) from 0 to 50% at fixed sputtering pressures of 3×10^{-3} and 16×10^{-3} Torr,

a series of a-C and a-C:N films were prepared. The N_2 gas flow rate was regulated between 0–21 and 0–96 sccm for the deposition pressures of 3×10^{-3} and 16×10^{-3} Torr, respectively, to reach the corresponding N_2% (percentage of nitrogen) in the sputtering gases. In the text, we use the terms films H and films L to represent the films prepared at the higher pressure (16×10^{-3} Torr) and the lower pressure (3×10^{-3} Torr), respectively. The films had similar thicknesses, of about 1 μm. At the experiment conditions, the non-nitrogenated (a-C) film L and film H had growth rates of approximately 250 and 210 Å min^{-1}, respectively, which are much slower than for the respective a-C:N films. The growth rates for a-C:N films varied from 260 to 420 and from 240 to 310 Å min^{-1} at 3×10^{-3} and 16×10^{-3} Torr, respectively; they also depend on the nitrogen ratios in the sputtering gases.

Fourier-transform infrared (FT-IR) spectroscopy (Nicolet Megna 760) and Raman spectroscopy (Renishaw 1000) were used to study the atomic bonding and structures of the films. FT-IR measurements on the films were performed in a reflectance mode. In the Raman system, a constant-wave green laser (514.5 nm) of about 3 mW power in a circular beam of about 2 μm diameter on the specimen surface was used. Each Raman spectrum was curve-fitted to two peaks (the D-peak and the G-peak) of a Gaussian distribution with a linear baseline. The film morphology was examined by atomic force microscopy (AFM, DI NanoScope III) in tapping mode.

Thermogravimetric analysis operating in dynamic and isothermal modes was performed with a DuPont 2100 thermogravimetric analyser (TGA 2950), which has a weight and temperature precision of ± 0.1 μg and ± 1 °C, respectively. The film/substrate composites of $\sim$15 mg were heated in a Pt pan in a closed furnace with a constant flow rate of air of 60 cm^3 min^{-1}. The dynamic TG experiment was conducted at a heating rate of 15 °C min^{-1} to a temperature at which the films were totally decomposed. The isothermal TG experiment was performed in a temperature range in which the films show dynamic decomposition, in order to study the kinetic decomposition processes. In the isothermal analysis, the initial specimens were heated at 200 °C min^{-1} to the designated temperature and maintained there for a period of time that varied from 15 to 65 min, depending on the weight losses of the films.

3. Results and discussion

3.1. Structure characterization

In all the a-C:N films, C–N, C=N, and C≡N bonds, corresponding to IR absorption centred at 1350, 1500, and 2200 cm^{-1}, respectively, were deduced from FT-IR spectra (figure 1). The frequencies and interpretations of these absorptions agree well with the literature [9, 17]. The intensities of these absorptions increased with the N_2%, indicating that more bonded nitrogen atoms were formed. Meanwhile, the fraction of unbonded molecules—especially N_2 molecules—might also increase as the N_2% increase. This is because the fraction of unreacted gaseous molecules which may get entrapped into the film structure increases with deposition pressure or N_2%. Raman measurements showed a significant band around 2320 cm^{-1} (the arrowed peaks in figure 2) for all the a-C:N films, which corresponds to the scattering of carbon nitride bonds, suggesting again the formation of carbon–nitrogen bonds in the a-C:N films. Beside carbon nitride peaks, figure 2 shows another obvious peak at around 700 cm^{-1} for most of the films, especially films L. This peak has been used to characterize a-C:N films with carbon–nitrogen bonds but its theoretical origin is still unclear [9]. Films H showed better resolved D-peaks and G-peaks than films L, which is a clear indication of higher graphitization in the structure of films H. The Raman spectra in figure 2 for the nitrogenated films of films H show increased background slopes, which is more obvious for a-C:N films of higher N_2%.

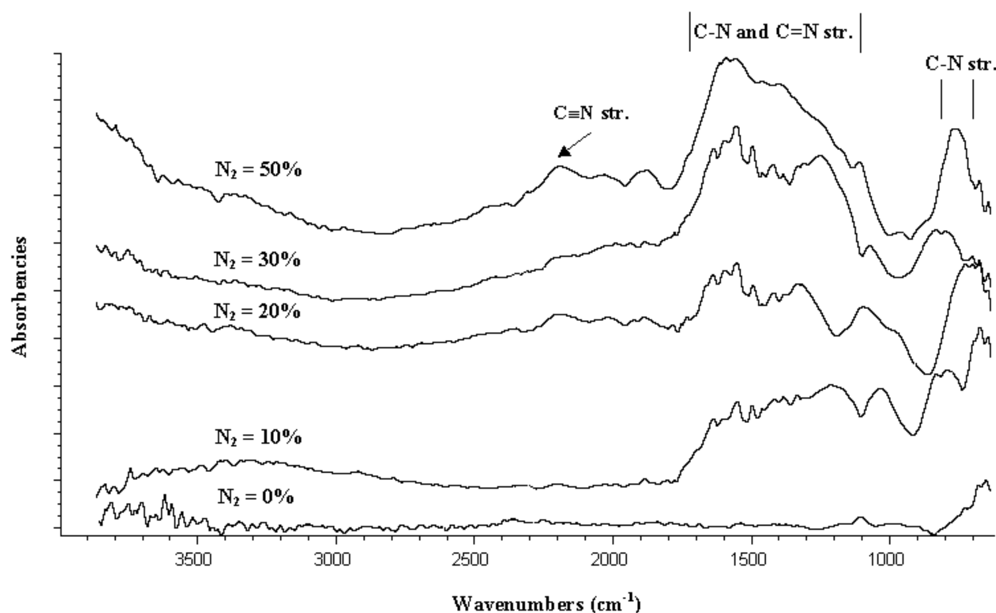

Figure 1. FT-IR spectra for films L with changing N_2% in the sputtering gases.

This is due to the stronger photoluminescence of the films. This phenomenon has been observed by other researchers and is quite similar to the case for hydrogenated films, in which an increased H% also led to stronger photoluminescence of the structure [18, 19]. Each Raman spectrum has a broad and skewed peak ranging from 1200 to 1700 cm^{-1}, which is composed of the overlapped D-peak (centred round 1300–1450 cm^{-1}) and the G-peak (centred round 1550–1580 cm^{-1}). The D-peak corresponds to the disorder mode of a graphitic structure belonging to the D_{6h}^{4} space group, while the G-peak is due to the E_{2g2} mode vibration of the graphitic structure [18]. The curve-fitted Raman data (figure 3) suggest that with the increase of the N_2% or the sputtering pressure, the G-peak shifted to higher frequencies while the D-peak shifted to lower frequencies. These are clear signatures of the structure graphitization increasing with the increase of the N_2% or the sputtering pressure [13]. These findings have been observed by other researchers and are considered to be due to the reduced energy of the carbon plasma at a higher sputtering pressure, which results in the reduction of the sp^3 fractions and increase in the content of unbonded molecules in the structure [19].

AFM measurements revealed that the surface roughness of the films increased with the sputtering pressure and the N_2% in the sputtering gases, which agrees with the findings in the literature [5–7, 18, 19]. This indicates that a more loosely bonded structure was formed at higher sputtering pressure or N_2%. There are three reasons for the increase of the surface roughness of the films with the sputter pressure or N_2%: first, increasing the sputtering pressure decreases the arrival energy of the atoms; second, the amount of entrapped gases in the films increases with pressure; third, the probability of interaction between the plasma and the film surface increases. Figure 4 shows typical surface topographies of AFM measurements over a 1×1 μm area, which have the same z-scale.

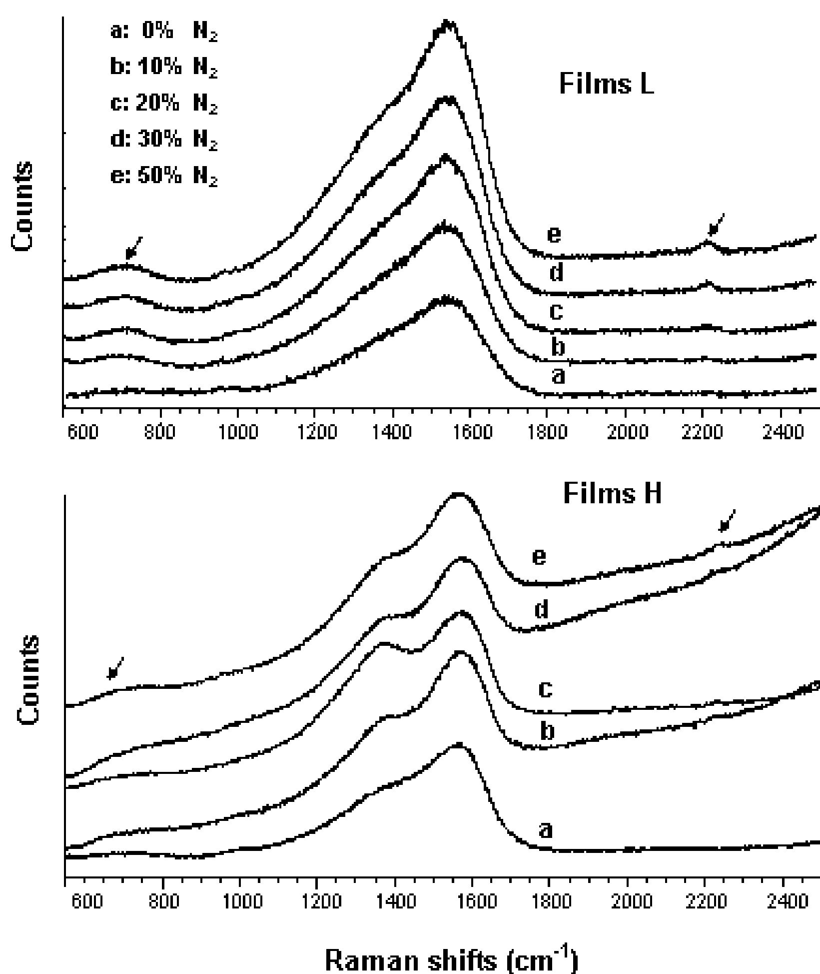

Figure 2. Raman spectra for films L and films H with changing N_2% in the sputtering gases. The arrowed positions at 2320 cm^{-1} and approximately 700 cm^{-1} indicate the scattering frequency of carbon nitrile and scattering characteristic of a-C:N films.

3.2. Dynamic TG analysis

A typical thermal decomposition process in an oxidizing atmosphere involves mass transfer, adsorption, desorption, and rearrangement. At low temperatures, the rate should be chemically controlled but may become diffusion controlled at high temperatures [16]. In the TG analysis, the flow rate of the air was fixed at 60 ml min^{-1} for all samples. The dynamic TG analysis indicates that the bare substrate showed a negligible weight loss of less than 0.05%, in contrast to the about 1% weight loss for the film/substrate samples. Owing to this, the dynamic weight-loss curves of the films were easy to obtain (figure 5). Typical DTG curves, expressed as rates of weight change (wt% min^{-1}) with temperature, are also presented in the insets of figure 5; their peaks correspond to decomposition of the main structures. The DTG data suggest that the decomposition is single step for films L while there are multiple overlapping steps for films H, indicating that films L have a highly integrated structure while the structures of films H are multiply packed [14]. The inset DTG curves in figure 5(*b*) can be divided into two peaks,

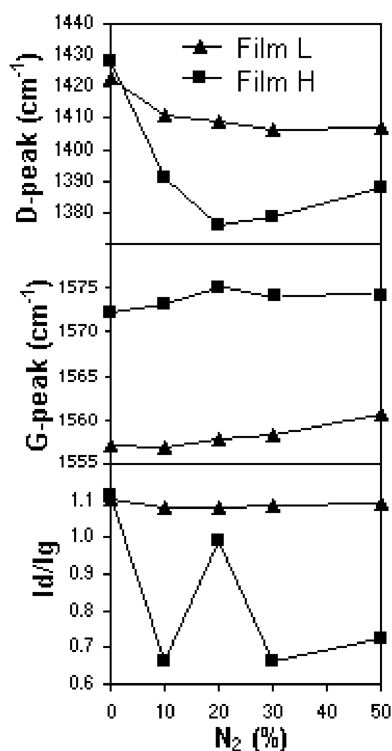

Figure 3. The D-peak frequencies, the G-peak frequencies, and their respective intensity ratios for the curve-fitted Raman spectra in figure 2.

centred at about 350 and 550 °C, and corresponding to the loss of loosely bonded molecules and the bonded main structure, respectively. The former process had a lower energy barrier than the latter one. This further confirmed that the content of loosely bonded molecules increased with the decrease of energy of the carbon plasma or the increase of the deposition pressure. The onset decomposition temperatures (T_{onset}) of the films from figure 5 are listed in table 1, which indicated that the a-C:N films had significantly higher thermal stability than the respective a-C films, but the stability does not consistently increase with the N_2%, as T_{onset} began to reduce when the N_2% reached 50%. The high stability of a-C:N is due to the higher dissociation energies of the carbon–nitrogen bonds that cross-link the structure matrix in a-C:N films as compared to carbon–carbon bonds in a-C films [20]. The thermal stability will be reduced by the presence of unbonded or loosely bonded small molecules entrapped in the structure, which escape easily at moderate heating, resulting in structure disintegration. The number of entrapped molecules increases with the sputtering pressure, while the number of entrapped N_2 molecules increases with the N_2% in sputtering gas for a-C:N films [19]. This explains the observation that films H showed lower thermal stability than films L, and the thermal stability of a-C:N films did not consistently increase with the N_2%. The weight losses before decomposition of the main structure, typically shown in the temperature range below 350 °C for films H and that below 400 °C for films L, are an indication of the unbonded small molecules lost at low heating temperatures [14].

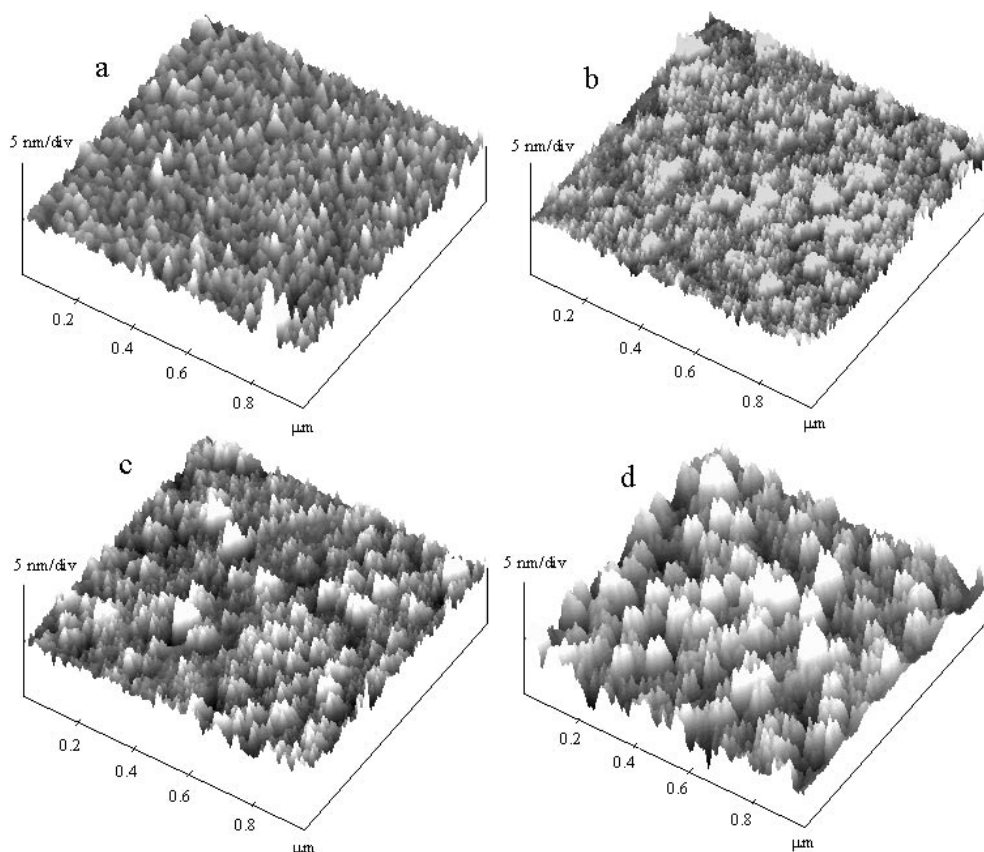

Figure 4. Typical AFM topography images for some a-C and a-C:N films. (*a*) Film L with 0% N_2; (*b*) film H with 0% N_2; (*c*) film H with 20% N_2; (*d*) film H with 50% N_2. The surface roughness increased with the increase of the sputtering pressure or the N_2% in the sputtering gases.

Table 1. The onset decomposition temperatures T_{onset} (°C) of a-C:N films with different percentages of N_2 in N_2/Ar during dc magnetron sputtering.

	3×10^{-3} Torr					16×10^{-3} Torr				
N_2	0%	10%	20%	30%	50%	0%	10%	20%	30%	50%
T_{onset}	396	502	545	538	481	340	380	365	360	355

3.3. Isothermal TG analysis

Isothermal analysis of the degradation of the a-C and a-C:N films was carried out in the temperature range of 350–575 °C to study the decomposition kinetics and possible mechanisms. Figure 6 shows two groups of isothermal curves, typical for films L and H, respectively. The weight-loss rate, r, can be obtained from the slope of the tangent to the isothermal curve corresponding to the particular time t. From the isothermal curves for films L, r gradually increased over time, giving convex-shaped curves (figure 6(*a*)). For films H, r reduced over time, resulting in concave-shaped curves. The change of r over time correlates well with the change of the apparent activation energy (ΔE), both reflecting the film structure difference.

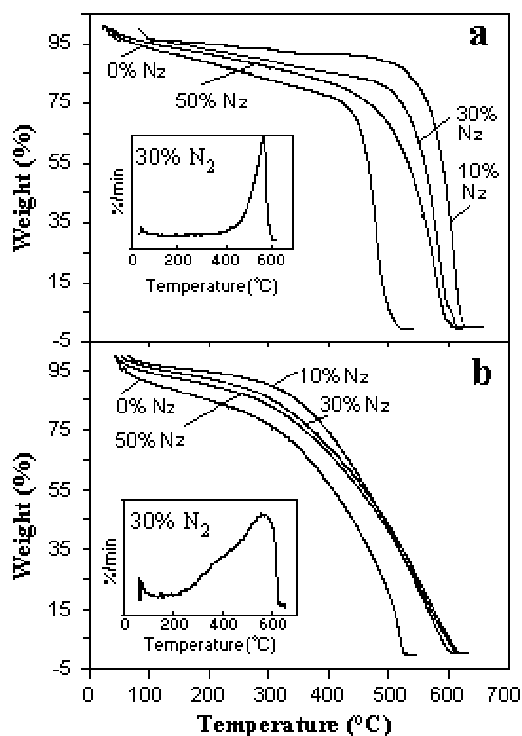

Figure 5. Dynamic TG curves for a-C and a-C:N films. (*a*) Films L, (*b*) films H. The insets show the differentials of the respective TG curves (DTG) for the a-C:N films sputtered in 30% N_2.

The values of the weight-loss rate, r, at different weight percentages of residue, expressed in % min^{-1}, were determined from the tangents to the isothermal curves.

The Arrhenius equation is normally used for calculating apparent activation energies of a reaction; it is expressed as

$$k = k_0 e^{-\Delta E/RT} \tag{1}$$

where k is the reaction rate constant, R the molar gas constant, and T the temperature in kelvins. k is related to reaction rate r by the expression

$$r = kf(1 - \alpha) \tag{2}$$

where α represents the reactant reacted at time t, $f(1 - \alpha)$ is a function of the reactant concentration at time t; it is the film thickness in this experiment. The value of ΔE for the decomposition process was hence determined by plotting $\ln(r)$ against the reciprocal of the temperature in kelvins (figure 7 and table 2). The choice of the expressions for $f(1 - \alpha)$ has little effect on the calculated results, since it is the natural logarithm of this quantity that is used.

From table 2, we see that all the films showed ΔE values that are slightly lower than that for the oxidation of carbon black in the chemically controlled temperature region [21], which is 230–270 kJ mol^{-1}. This suggests that the sputter-coated amorphous films might be thermally less resistant than carbon black for reasons such as gaseous molecules being entrapped in the structure. The data in table 2 also indicate that a-C:N films show significantly higher ΔE values than the respective a-C films—caused by the higher dissociation energies

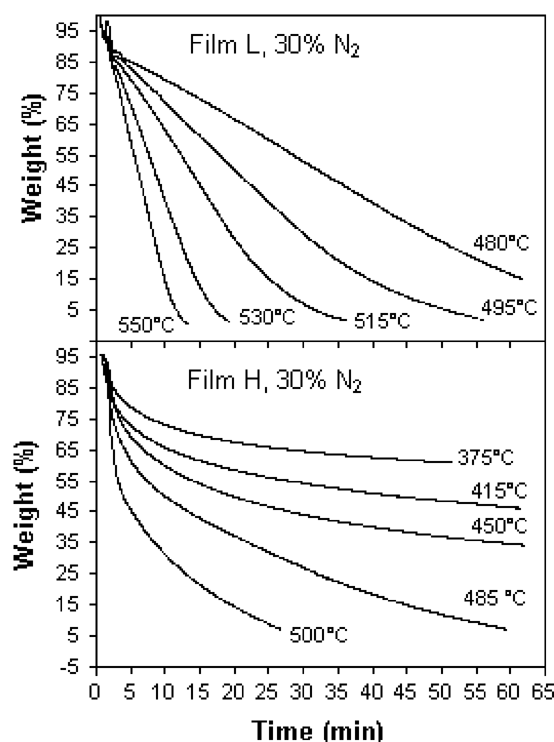

Figure 6. Typical isothermal weight-loss curves at different temperatures for the a-C:N films deposited at 30% N_2 at two different sputtering pressures corresponding to films L and H.

Table 2. Summary of ΔE (kJ mol^{-1}) values calculated from $\ln(r) \sim 1/T$ plots for the decomposition a-C:N films sputtered with various percentages of N_2 in N_2/Ar at pressures of 3×10^{-3} and 16×10^{-3} Torr, respectively. R (wt%) is weight percentage of the residue.

	3×10^{-3} Torr			16×10^{-3} Torr		
R (wt%)	0% N_2	10% N_2	30% N_2	0% N_2	30% N_2	50% N_2
75	149	154	155	95.9	138	120
65	141	154	153	98.8	141	116
55	138	147	152	104	145	125
45	126	133	141	117	156	126

of the carbon–nitrogen bonds that cross-link the structure matrix. During film deposition, a higher sputtering pressure yields lower energies of carbon plasma, resulting in an increase in the content of unbonded or loosely bonded molecules [19,22], which is detrimental to thermal stability. The change of ΔE with the film loss in wt% explains, to some extent, the change in thermal stability of the films during decomposition. Within a certain range, a gradual decrease of ΔE with the amount of weight loss (wt%) is observed for films L, while an increase of ΔE with the amount of weight loss (wt%) is observed for films H.

Thermal dissociation is, in general, an endothermic process; the processes with lower energy barriers or ΔE happened at lower temperatures. A decrease of ΔE with the amount of decomposed product is a common phenomenon in thermal decomposition—meaning that the structure gradually loses thermal stability as the reaction progresses. The films produced with

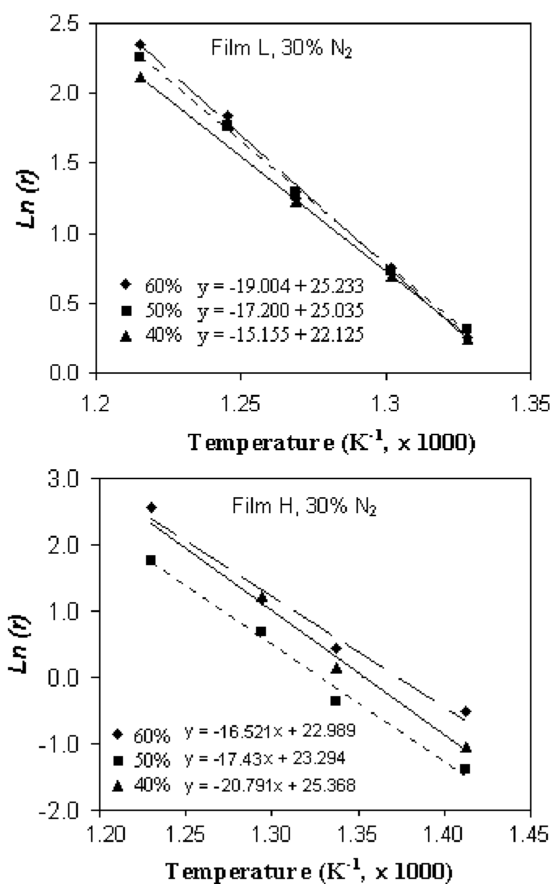

Figure 7. Typical $\ln(r)$ versus $1/T$ plots for a-C:N films deposited at 30% N_2 at two different sputtering pressures corresponding to films L and films H.

higher-energy carbon plasma (films L) had higher degrees of structural integration or initial ΔE and were more resistant to thermal dissociation. Once the decomposition was initiated, the structure integration was destroyed, resulting in a gradual decrease of ΔE with the amount of weight loss (wt%). The decrease in ΔE leads to an increase in r with t according to the Arrhenius equation (equation (1)), which correlates with the slightly convex shape of the isothermal curves (figure 6(*a*)). The increase of ΔE with the amount of weight loss that was observed for films H could be due to different reactions within the weight-loss range studied. The loss of loosely bonded molecules had a lower energy barrier or ΔE, and took place at lower temperatures (figure 5(*b*)). With the increase of temperature, the bonded structure began to decompose—which had a higher energy barrier or ΔE, and therefore led to a phenomenon of increasing ΔE with film loss in wt%. From equation (1), this indicates an exponentially reduced r, correlating with the concave-shaped isothermal curves (figure 6(*b*)).

To analyse the reaction mechanisms, the r-values (wt% min^{-1}) were determined at different times from the isothermal curves (figure 6). Here, α is used to represent the fraction of the solid decomposed at time t, k is the rate constant which is related to temperature by the Arrhenius equation $k = k_0 e^{-\Delta E/RT}$, and $g(\alpha)$ is a function of α (it depends on the decomposition mechanism): $g(\alpha) = kt$. Some very frequently used models, including

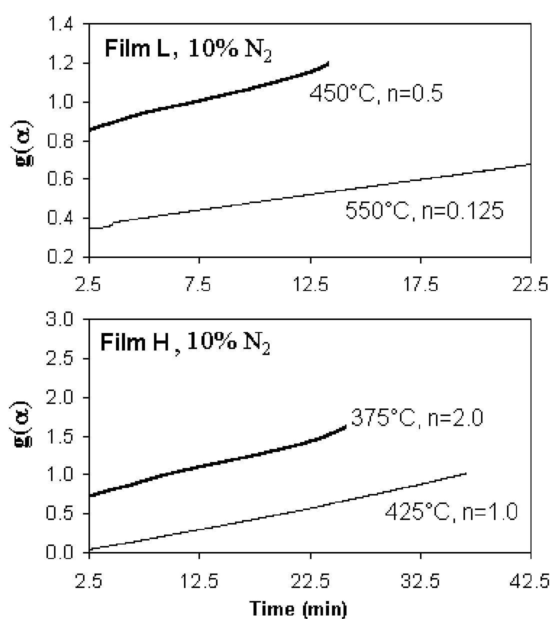

Figure 8. Typical $g(\alpha)$ versus t plots for a-C:N films deposited at 10% N_2 at two different sputtering pressures corresponding to films L and films H.

first-order and diffusion-controlled kinetics, were proposed to explain mechanisms of solid-state decomposition [23]. After fitting the isothermal data into the models, it was found that the reactions could best be represented by nth-order reactions, or $g(\alpha) = -[\ln(1 - \alpha)]^n$, where n is the apparent reaction order. Figure 8 shows some typical $g(\alpha)$ versus t plots. The first-order reaction ($n = 1$) is the simplest process. For bulk materials, the reaction is chemically controlled at low temperatures but diffusion controlled at high temperatures, corresponding to a reduced n at higher temperatures. Therefore, the value of n depends on the film structure and the reaction temperature. In the experiment, the value of n varied from 0.125 to 2. Films L generally had smaller n-values than the corresponding films H, and the reaction at high temperatures had smaller n-values. This indicates that the reactions were affected by product diffusions even for the films of about 1 μm thickness. As discussed above, the films prepared with higher-energy carbon plasma (films L) had higher packing density and decomposition temperature; they are expected to have lower reaction orders because of the slow diffusion rate of the product caused by the densely packed structure. Again, the difference in n-value is associated with the thermal stability of the films; a structure with high packaging density and thermal stability showed low apparent reaction order.

4. Conclusions

The study has shown that the onset decomposition temperatures for amorphous carbon films were significantly increased for nitrogenated structure and when high-energy carbon plasma was used during film deposition. In response to the improved thermal stability, the apparent activation energy for thermal decomposition was also increased. The changes of ΔE with the weight percentage and decomposition rate with time are associated with the physicochemical changes in the structures during decomposition. The films of higher packing density and structural integration, achieved by using high-energy carbon plasma,

showed a gradually accelerated single-step decomposition due to loss of thermal stability with decomposition, corresponding to a reduced ΔE with an exponential weight percentage increase in decomposition rate. The presence of unbonded and loosely bonded molecules due to the use of low-energy carbon plasma at a higher deposition pressure is indicated by the thermal analysis. The loss of unbonded molecules had lowest energy barrier or ΔE and happened before the main structure decomposition, including the loss of bonded molecules. The loss of loosely bonded molecules had a lower ΔE which overlapped with those for the bonded ones, leading to a two-step decomposition. The decomposition mechanisms can best be expressed using nth-order reactions, $-g(\alpha) = [\ln(1 - \alpha)]^n$, with the value of the apparent reaction order n changing from 0.125 to 2, depending on the film structure and reaction temperature. The films of high packing density and thermal stability showed lower n-values than the films with high contents of loosely bonded compositions. In all cases, the decompositions were controlled by the diffusion at higher temperatures.

Thermal properties of a-C and a-C:N films were investigated, compared, and explained in relation to the structural basis of the films. These properties are also closely related to other properties such as mechanical, electrical, optical, and especially tribological properties of the films. Examining the tribological properties and correlating them with the thermal behaviours of the films would be an interesting research aim to pursue.

References

[1] Liu A Y 1994 *Phys. Rev.* B **50** 10 362
[2] Muhl S and Méndez J M 1999 *Diamond Relat. Mater.* **8** 1809
[3] Xiao X C, Jiang W H, Song L X, Tian J F and Hu X F 1999 *Chem. Phys. Lett.* **310** 240
[4] Bhushan B 1999 *Diamond Relat. Mater.* **8** 1985
[5] Bhattacharyya S, Cardinaud C and Turban G 1998 *J. Appl. Phys.* **83** 4491
[6] Wang D F, Kato K and Umehara N 2000 *Surf. Coat. Technol.* **123** 177
[7] Tessier P Y, KreN'guessan R, Angleraud B, Fernandez V, Mubumbilia N and Turban G 2000 *Surf. Coat. Technol.* **125** 295
[8] Cutiongco E C, Li D, Chung Y W and Bhatia C S 1996 *J. Tribol.* **118** 543
[9] Neuhaeuser M, Hilgers H, Joeris P, White R and Windeln J 2000 *Diamond Relat. Mater.* **9** 1500
[10] Wei B, Zhang B and Johnson K E 1998 *J. Appl. Phys.* **83** 2491
[11] Zhang L H, Gong H and Wang J P 2001 *J. Phys.: Condens. Matter* **13** 2989
[12] Tallant D R, Parmeter J E, Siegal M P and Simpson R L 1995 *Diamond Relat. Mater.* **4** 191
[13] Dillon R O, Woollam J A and Katkanant V 1984 *Phys. Rev.* **29** 3482
[14] Speyer and Robert F 1994 *Thermal Analysis of Materials* (New York: Dekker)
[15] Wang D Y, Chang C L and Ho W Y 1999 *Surf. Coat. Technol.* **120–1** 138
[16] Levenspiel O 1999 *Chemical Reaction Engineering: An Introduction to the Design of Chemical Reactors* (New York: Wiley)
[17] Vien L D, Colthup N B, Fateley W G and Grasselli J G 1991 *The Handbook of Infrared and Raman Characteristic Frequencies of Organic Molecules* (San Francisco, CA: Academic)
[18] Yoshikawa M 1989 *Mater. Sci. Forum* **52&53** 365
[19] Spaeth C, Kühn M, Richter F, Falke U, Hietschold M, Kilper R and Kreissig U 1998 *Diamond Relat. Mater.* **7** 1727
[20] *CRC Handbook of Chemistry and Physics* 1985 65th edn, ed R C Weast, M J Astle and W H Beyer (Boca Raton, FL: Chemical Rubber Company Press)
[21] Marsh H I 1989 *Introduction to Carbon Science* (Oxford: Butterworth)
[22] Stanishevsky A 1998 *Mater. Lett.* **37** 162
[23] Shlensky O F, Askenov L N and Shashkov A G 1991 *Thermal Decomposition of Materials—Effect of Highly Intensive Heating* (Amsterdam: Elsevier)